Volume 79 • Issue 1 • November 2016

Journal of Achievements in Materials and Manufacturing Engineering

International Scientific Journal published monthly by the World Academy of Materials and Manufacturing Engineering

Synthesis and characterization of NiO-ZnO nanocomposite by a cost efficient self-combustion technique

M. Vimal Kumar, T.S. Gokul Raja, N. Selvakumar *, K. Jeyasubramanaian

Centre for Nanoscience and Technology, Department of Mechanical Engineering,
Mepco Schlenk Engineering College, Sivakasi, Tamil Nadu 626005, India
* Corresponding e-mail address: nselva@mepcoeng.ac.in

ABSTRACT

Purpose: In this research work the nickel oxide incorporated zinc oxide nano composite with various level of percentage such as (0.2, 0.4 and 0.6) were synthesized using combustion processes. Fuel used for the combustion process is hexamine in this work. Oxidizing agents taken were the nitrates of zinc and nickel. These precursor nitrates were heated with hexamine fuel to undergo combustion process.

Design/methodology/approach: After combustion the particles were collected and heat treated to maintain the purity of the samples. XRD results were in well accordance with the JCPDS data and the average crystalline sizes were in the range of 10~20 nm. UV-VIS absorbance results confirm the band gap in the visible region. With increase in concentration of NiO in the composite red shifted from 320 nm to 374 nm. FTIR supports the presence of Zn-O and Ni-O bonds by the characteristic vibrational peaks at 432 cm^{-1} and 470 cm^{-1} respectively. PL spectrum studies results in the redshift of ZnO peaks from 380 nm to 400 nm with addition of Ni^{2+} ions inside the lattice. SEM and AFM studies reveals the morphological and topographical visualizations of the nanocomposite powders.

Findings: In this research work, the authors had successfully synthesized Nickel substituted Zinc oxide by following simple combustion method followed by annealing. XRD analysis clearly evidences the formation of ZnO in the hexagonal wurtzite structure with an average crystallite size of 15 nm to 18 nm. An increase in Nickel peaks in between the Zinc oxide peaks were observed with increase in the nickel concentration in the composition.

Practical implications: We conclude that combustion technique is suitable to fabricate Nickel incorporated Zinc oxide particles with high purity. This powder can be used in transparent conducting thin flims for OLED applications.

Keywords: NiO-ZnO nano composites; Photoluminescence; XRD refinements

Reference to this paper should be given in the following way:

M. Vimal Kumar, T.S. Gokul Raja, N. Selvakumar, K. Jeyasubramanaian, Synthesis and characterization of NiO-ZnO nanocomposite by a cost efficient self-combustion technique, Journal of Achievements in Materials and Manufacturing Engineering 79/1 (2016) 13-18.

MATERIALS

1. Introduction

In recent years, materials possessing different anomalous properties are the current trend of research. Many researchers over the world are working on this basis to find out new materials with different properties. In this aspect, semiconducting materials with different outstanding properties were fabricated by various research groups. A better field in this aspect of the investigation work is materials possessing both semiconducting properties and magnetic properties. If a semiconductor is doped with a certain amount of transition metal atoms like Ni, Co, Al, Fe, Cu, Co, Mn and V shows a new property in the semiconducting device as a magnetic material. It means that the material with these doping, depending upon the levels of doping can make the semiconductor to behave as a magnet. These properties can be used for magnetic random access memory (MRAM) device. However, x-ray diffraction studies of these materials have not been reported by any researchers till now. Our focus of work is to investigate the variation in the lattice parameters of the semiconducting material when it got doped with a TMA (Transition metal atoms) In our current work, nickel incorporated zinc oxide was extensively studied for its fascinating properties like diluted magnetic semiconductor (DMS). As a low cost material, nickel-doped zinc oxide have been widely studied for its wide range of applications in Spintronics, Diluted magnetic semiconductors (both semiconducting and magnetic property), Transparent electronic devices, gas sensor, solar cell, piezoelectric transducer, magnetic FET's, electrochromic devices, smart window, UV-detectors, surface acoustic wave device, LED's, laser diode, UV protection cosmetics, photocatalytic process, and also to avoid photo-corrosion of ZnO under UV radiation while doping with Ni [1-6].

2. Materials and methods

If in our work, nickel oxide incorporated zinc oxide nanocomposite powders were synthesised by a simple combustion process. Zinc nitrate hexahydrate (Merck, 99% pure), Nickel (II) nitrate hexahydrate and Hexamine (Merck, 99%) were fixed as the precursors for the process. Appropriate amounts of Nickel precursor (0.6M, 0.4M & 0.2M) were dissolved in 10ml of distilled water. Fixed amount of zinc precursor is also dissolved in 10ml of distilled water. After achieving transparency, the two solutions were stirred magnetically for 10min to form a precursor solution. 3g of hexamine is mixed with the precursor solution, followed by an agitated stirring for 30 min. PEG (4000) is dissolved in 5 ml of distilled water separately. After dissolution PEG is introduced into the precursor solution. After 10 min of stirring 65 drops of Ammonia solution is added into the solution, in this case, the pH of the solution is tuned to 9. Now the beaker containing the solution is heated on a hot plate of 120°C. After 30 min the solution gets transformed to gel and within another 10 min combustion starts with the evolution of fumes. At the case of complete combustion, brown coloured fibrous particles were left out in the beaker. This intermediate product is scrapped and annealed in a tubular furnace at 500°C for 2 hrs. The synthesised nanomaterials were then subjected to characterization studies. X-ray diffraction studies were done using an X-ray Diffractometer. FTIR spectra of the samples were recorded using Alpha FTIR Spectrometer. UV-vis absorption studies were done using Lambda 25 UV/Vis spectrometer. Photo-luminescence spectra were measured from spectrofluoro-photometer. SEM images were collected from SUI510 Scanning Electron Microscope. The topography of the samples was recorded using AFM.

3. Results and discussion

3.1. XRD studies

Different nanopowders of composition $ZnNi_xO$ (x=0, 0.2, 0.4, 0.6) have been exposed to monochromatic X-rays and the resulting diffraction patterns were shown in figures. Set of diffraction peaks located at 32, 34, 48, 67, 53, 66, 67, 68, 73 and 77 were corresponding to (100), (002), (102), (110), (103), (200), (112), (201), (004) and (202) planes respectively. These are the characteristic peaks of ZnO which gets crystallize in hexagonal Wurzite structure and its match the JCPDS file of 891397.Another set of three diffraction peaks arised over 37.243, 43.289 and 75.2 were corresponding to (003), (012), and (113) planes respectively. These peaks get originated due to the formation of rhombohedral NiO in the compound and its match with the JCPDS 897390 (Table 1).

Table 1.
XRD values of NiO

X	Compound	a	c	D, nm
0.2	NiO	2.954	7.290	17.07
0.4	NiO	2.957	7.276	15.01
0.6	NiO	2.958	7.247	16.68

Many studies in this compound ends within 10% of Ni doping. 10% is the maximum solubility limit of Ni in the ZnO lattice. Above this percentage further studies have not been reported till now.

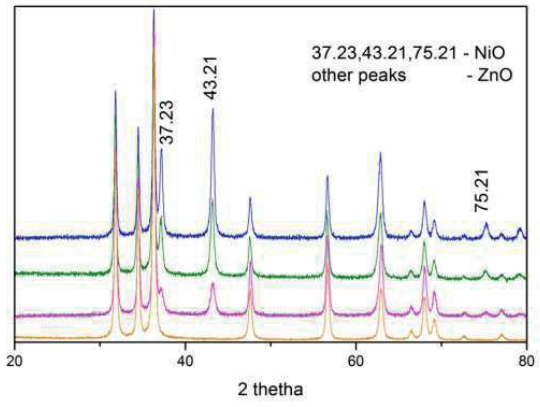

Fig. 1. XRD pattern of nickel incorporated zinc oxide

The variation in lattice parameters of the Ni doped ZnO were shown in Table 2. Up to 40% Ni doping in the ZnO composition, an increase in the lattice constants of ZnO was observed. A substitution of the Ni on the Zn site contributes this lattice shifting behaviour. Beyond that limit lattice constant is again decreasing. This may arise due to the formation of NiO along with the ZnO compound. A view on NiO lattice constants clearly shows a increment in 'a' and decrement in 'c' along their axes. Refinement procedure was done for all the four xrd values using Jana 2006 software. Resulting graph showing the observed values, calculated values and their difference values were shown in Fig. 1.

Table 2.
XRD values of ZnO

X	Compound	a	c	D, nm
0	ZnO	3.2446	5.1981	20.35
0.2	ZnO	3.2477	5.2014	22.38
0.4	ZnO	3.2478	5.2036	23.56
0.6	ZnO	3.2453	5.1982	23.61

3.2. FTIR spectra analysis

FTIR spectrum of Nickel doped zinc oxide nano particles at room temp is shown in the Fig. 2. The spectrum was recorded in the range of 4000 cm^{-1}-400 cm^{-1}. The spectrum did not show any characteristics peaks in the range of 500 cm^{-1}-4000 cm^{-1}. This revealed that the synthesized particles were metallic in nature and it showed that the sample contains no impurity. FTIR spectroscopic analysis of the four samples was done and the resulting transmittance spectra were plotted in fig. Peaks originated nearer to 470 cm^{-1} were corresponding to Nickel-oxygen vibrations [7]. Peaks visible at 432 cm^{-1} is due to the stretching frequency of ZnO [8]. Strong peaks at 457-462 cm^{-1} is due to the vibrations assigned due to ZnO [8].The same chemical compositions were confirmed by the XRD pattern.

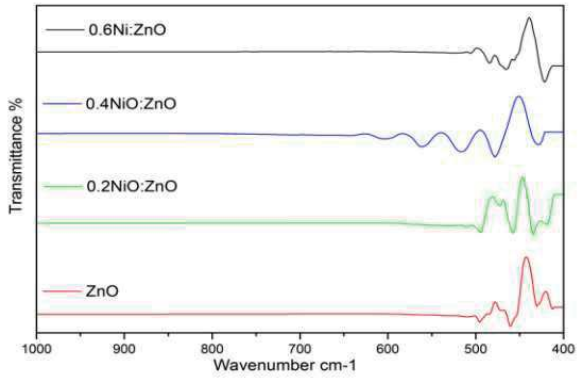

Fig. 2. FTIR spectrum of nickel incorporated zinc oxide

3.3. UV-VIS spectrum analysis

The optical absorption spectrum of nickel nanoparticles is observed in Fig. 3. It can be seen that the strongest absorption peak of the as-prepared sample appears at around 360-370 nm [9].

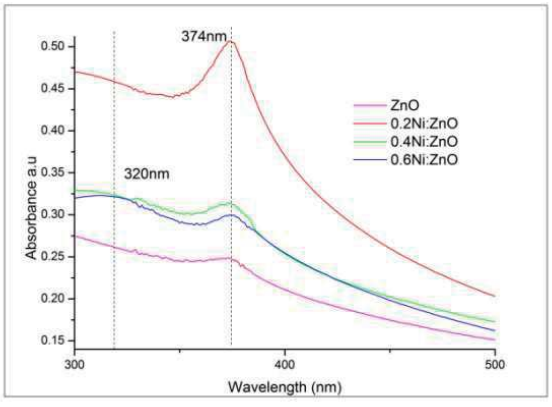

Fig. 3. UV-vis spectrum of nickel oxide incorporated zinc oxide nanocomposite

The observed red shift in the absorption band edge with nickel doping in ZnO may be due to the sp-d exchange interactions between the band electrons and the localized d-electrons of the Ni^{2+} ions[10]. Such a red shift in and edge with increasing nickel dopant is a clear indication for the incorporation of Ni ions into the Zn site of the ZnO lattice. It is observed that the absorption spectrum of nickel incorporated ZnO Nano particle shows additional absorption bands corresponding to d–d transitions. The reason for red shift in band edge is due to the change of the sp–d exchange interactions between the band electrons and the localized d-e^- of the Ni^{2+} ions which is also considered as the blossoming of magnetic phase.

3.4. Photoluminescence spectroscopy

This analysis was carried out using Fluoro Max-4 Spectrofluorometer. It shows broad band emission between 500 to 600 nm which is due to deep level emission. Emission peak is observed at compared to bulk nickel incorporated zinc oxide at 408 nm [8]. The main difference between these two samples is that Ni^{2+} doping concentration in $Zn_{0.98}$ $Ni_{0.02}O$ nanoparticles obtained in air atmosphere decreases. As mentioned above Ni doping in ZnO results in a redshift of UV emission in comparison with pure ZnO due to the incorporation Ni ions into Zn lattice to replace Zn ions. Two emission bands appear in the PL spectra. One is ultraviolet (UV) band around 400 nm, which is attributed to band edge exciton recombination. Obviously, Ni doping in ZnO results in a red shift of UV emission in comparison with pure ZnO (380 nm) due to the incorporation of Ni ions into the Zn site of the ZnO lattice (Fig. 4).

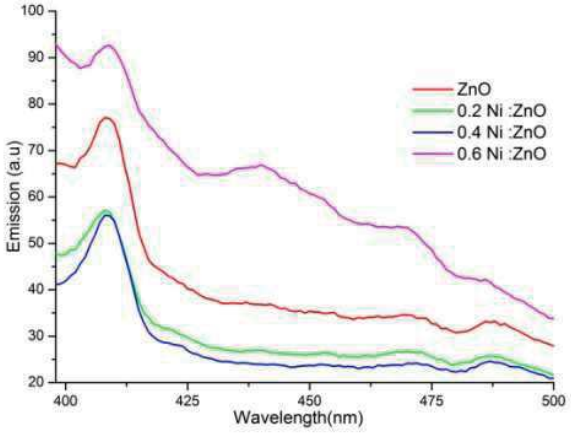

Fig. 4. Photoluminescence spectra

3.5. SEM image analysis

The surface morphological features of synthesized nanoparticles were studied by scanning electron microscope. Figure 5 shows the SEM image of Ni nanoparticles with magnification of 3000x. The other instrumental parameter such as accelerating voltage, spot size and working distances were indicated on the SEM image. The results indicated that mono-dispersive and porous Nickel incorporated zinc oxide nanoparticles were obtained. The SEM observations of the sample reveal that the shape of the Ni incorporated zinc oxide particles of various doping percentage such as (0.2, 0.4, 0.6) was spherical. The observation of some larger nanoparticles may be attributed to the fact that Nickel incorporated zinc oxide nanoparticles have the tendency to agglomerate due to their high surface energy and high surface tension of the ultrafine nanoparticles and also have been resulted from magnetic interaction and polymer adherence between the particles. It is proved from the above images that, porous nano structured oxide type materials can be easily synthesized from the hexamine combustion process. If an optimization of this process is done in a perfect manner, size of these pores can be controlled. This makes use of this nanomaterial in a wide range of applications such as sensors, nano filters and superhydrophobic materials. Nickel particles are seemed to be spread over the zinc oxide compound. It can be concluded that the prepared Nickel incorporated zinc oxide particles are in nanometer range.

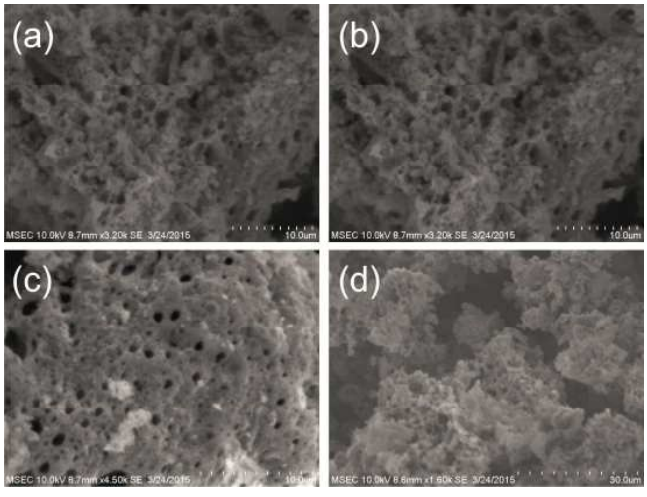

Fig. 5. SEM image of nickel (0, 0.2, 0.4, 0.6) incorporated zinc oxide nanoparticles

3.6. AFM analysis

AFM provides a 3D profile of the surface on nanoscale, by measuring forces between a sharp probe and surface at very short distance. The probe is supported on a flexible cantilever. The size of the particle was observed by scanning a glass slide coated with the synthesized nickel incorporated zinc oxide nanoparticles. The AFM image was processed using XEI software and the 3D profile analysis of the image was done. Images were collected by fixing the scanning range of 10 µm x 10 µm. Scan rate is fixed for all the samples as 0.5 Hz. Non-contact mode was chosen to collect the surface topography of the nanomaterial, as the surface roughness is higher. A wide range in the height of the particles is obtained as 100 nm to 400 nm. From the 3D profile analysis, size of the particles was found around 100 nm. 0%, 40% and 60% nickel in the zinc oxide compound shows an agglomeration and particle sizes between 100 nm-200 nm. Even distributions of particle with lesser sizes were observed in all the compounds. This is due to the fact that Zinc oxide nanomaterial gets evenly crystallized at 500°C. As the concentration of Nickel in the zinc oxide matrix is lesser they get floated over the zinc oxide matrix with particle sizes ranging up to 400 nm (Fig. 6).

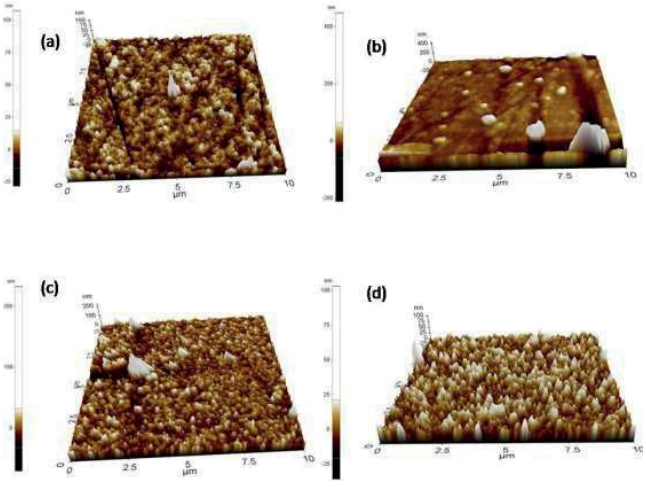

Fig. 6. AFM image of nickel (0, 0.2, 0.4, 0.6) incorporated zinc oxide nanoparticles

This is in paradox with the average crystalline size obtained from the X-ray diffractions. 15 nm to 18 nm crystallite sizes have been obtained from XRD, while a huge deviation in the particle sizes can be visualized through AFM. SEM analysis is a evidence for the floating nickel particles in larger sizes than the zinc oxide matrix. As the ratio of sizes obtained from SEM and XRD is found to be higher than one, polycrystallinity and agglomeration of these magnetic materials can be proved to be true. As the concentration of the Nickel in the zinc oxide gets increases, the even distribution of these larger particles over the base compound can be seen with its higher height in all the images. Thus a difference in height confirms the presence of Nickel oxide nanoparticles over the zinc oxide compound using AFM.

4. Conclusions

In this research work, the authors had successfully synthesized Nickel substituted Zinc oxide by following simple combustion method followed by annealing. Nickel doping concentration has been varied from 0.02 to 0.08 with respect to Zinc oxide in the composition. The as synthesized powders were further studied with XRD, SEM, AFM, and FTIR analysis. XRD analysis clearly evidences the formation of ZnO in the hexagonal wurtzite structure with an average crystallite size of 15 nm to 18 nm. An increase in Nickel peaks in between the Zinc oxide peaks were observed with increase in the nickel concentration in the composition. AFM analysis reveals the average particle size in the range of 100 nm-400 nm. SEM analysis confirms the presence of spherical shaped particles uniformly distributed over the surface. Hence, we conclude that combustion technique is suitable to fabricate Nickel incorporated Zinc oxide particles with high purity. This powder can be used in transparent conducting thin films for OLED applications.

References

[1] Jinping Liu, Chuanwei Cheng, Weiwei Zhou, Hongxing Li and Hong Jin Fan, Ultrathin nickel hydroxidenitrate nanoflakes branched on nanowire arrays for high-rate pseudocapacitive energy storage, Chemical Communications 47 (2011) 3436-3438.

[2] Juan Xie, Yanting Li, Wei Zhao, Li Bian, Yu Wei, Simple fabrication and photocatalytic activity of ZnO particles with different morphologies, Powder Technology 207/1–3(2011) 140-144.

[3] L.Q. Jing, Y.C. Qu, B.Q. Wang, S.D. Li, B.J. Jiang, L.B. Yang, W. Fu, H.G. Fu, J.Z. Sun, Review of photoluminescence performance of nano-sized semiconductor materials and its relationships with photocatalytic activity, Solar Energy Materials Solar Cells 90 (2006) 1773-1787.

[4] X.T. Zhang, D.A. Tryk, Heterogeneous photocatalysis: fromwater photolysis to applications in environmental cleanup, International Journal of Hydrogen Energy 32 (2007) 2664-2672.
[5] O.S. Mohamed, S.A. Ahmed, M.F. Mostafa, A.A. Abdel-Wahab, Nanoparticles TiO2-photocatalyzed oxidation of selected cyclohexyl alcohols, Journal of Photochemistry and Photobiology A 200 (2008) 209-215.
[6] A.O. Ibhadon, G.M. Greenway, Y. Yue, P. Falaras, D. Tsoukleris, The photocatalytic activity and kinetics of the degradation of an anionic azo-dye in a UV irradiated porous titania foam, Applied Catalysis B 84 (2008) 351-355.
[7] S.L. Hunte, An overview of semiconductor photocatalysis, Journal of Photochemistry and Photobiology A 108 (1997) 1-35.
[8] G. Riegel, J.R. Bolton, Photocatalytic efficiency variability in TiO2 particles, The Journal of Physical Chemistry 99 (1995) 4215-4224.
[9] V.D. Mote, Y. Purushotham, B.N. Dole, Williamson–Hall analysis in estimationof lattice strain in nanometer-sized ZnO particles, Journal of Theoretical and Applied Physics 6/6 (2012) 2251-7235.
[10] P. Pandey, N. Singh, F.Z. Haque, Development and optical study of hexagonalmulti-linked ZnO micro-rods grown using hexamine as capping agent, Optik124 (2013) 1188-2119.
[11] M. Rezaei, A.H. Yangjeh, Simple and large scale refluxing method for prepara-tion of Ce-doped ZnO nanostructures as highly efficient photocatalyst, Applied Surface Science 265 (2013) 591-596.
[12] O. Singh, M.P. Singh, N. Kohli, R.C. Singh, Effect of pH on the morphology andgas sensing properties of ZnO nanostructures, Sensors and Actuators 166-167 (2012) 438-443.
[13] K. Vanheusden, C.H. Saeger, W.L. Warren, D.R. Tallant, J.A. Voight, Correlation between photoluminescence and oxygen vacancies in ZnO phosphors, Applied Physics Letters 68 (1996) 403-405.
[14] T. Al-Harbi, Hydrothermal synthesis and optical properties of Ni doped ZnOhexagonal nanodiscs, Journal of Alloys and Compounds 509 (2011) 387-390.
[15] A.K. Zak, W.H.A. Majid, M.E. Abrishami, R. Yousefi, X-Ray analysis of ZnOnanoparticles by Williamson–Hall and size-strain plot methods, Solid State Sciences 13 (2011) 251-256.